ASIAN JOURNAL OF CIVIL ENGINEERING (BUILDING AND HOUSING) VOL. 6, NO. 6 (2005)
PAGES 511-532

A STUDY OF POWER TRANSMISSION POLES

M. Ashraf*, H.M. Ahmad and Z.A. Siddiqi
Department of Civil Engineering, University of Engineering and Technology
Lahore, Pakistan

ABSTRACT

An in-depth study into behaviour of high voltage transmission poles has been made covering their loading, analysis and design aspects. Due to large displacements produced, the secondary effects have to be accounted for in the solution of pole structure. Therefore, it becomes necessary to consider the geometric non-linearity while analysing a pole.

The development of a new and efficient technique was considered necessary due to limitations of available methods of analysis for pole structures. For this purpose, "*tapered modelling technique*" has been introduced by the authors. The finite element method, considered to be providing exact solution, is based on use of thin shell elements, requires a considerably large computer time and memory. Other available modelling techniques are based on frame elements, solutions of which are not found in good agreement with the exact solution unless nodes selected are appreciably high in number.

In this work, the analysis of poles is carried out by tapered model along with one of the standard packages based on finite element method. It is gratifying to note that the results obtained from developed tapered model are observed to be having close agreement with those of exact method.

Keywords: Modelling technique, tower, pole, standard packages

1. INTRODUCTION

The lattice skeletal towers are being employed for transmission lines almost since the beginning of this industry. During the last two or three decades, the use of steel pole structures for this purpose is started and their use is increasing rapidly. With the growing demand, a considerable increase in the number of manufacturers with new configurations of poles and towers has occurred. They are also equipped with new design, fabrication and erection techniques of these structures.

Poles are considered better than towers due to their following advantages:

1. Poles can be erected on relatively much smaller space. As a result of this, these are cheaper and better compared with those of towers in cities, where limited right of way is expensive.

* Email-address of the corresponding author: dr_mashraf@msn.com

2. Corrosion of a certain vital member of a tower or lose of a single bolt may lead to failure of whole structure. On the contrary, local damage to a pole is bridged over due to continuum type of structure.
3. Poles are subjected to lesser wind loads as compared to towers due to smaller aerodynamic coefficient, thus economizing their use.
4. Poles, being a continuum type, offer more resistance to terrorist activities compared with those of towers.

This research work is aimed at bringing together the more pertinent aspects of analytical techniques on which steel pole design is carried out and its direct application to high voltage power transmission lines. The recommendations made as a result of this work have been developed to relate primarily to high or extra high voltage transmission lines (100 KV and above) where reliability and continuity of service must be provided. As the need for electric power increases and available right-of-way becomes more critical in term of cost and space particularly in cities, the demand for pole type structures will enhance with passage of time.

The routine analysis of polygonal masts is carried out by considering the uniformly tapered pole as a telescopic mast with abrupt cross-sectional variations (Fig- 1c). Despite the fact that this approach does not represent its true simulation, the professionals rely on this technique for convenience in its modelling by employing the prevailing structural software. The cost of over-designing as opposed to the risk of under-designing transmission line structures for longitudinal strength has become a serious concern for design engineers.

A little saving in a single pole structure on the basis of certain design evidence may lead to an appreciable reduction in the cost of total project due to the presence of their large number in an electric line. This depicts their importance and necessitates their analysis and design on the basis of such techniques, which should give the best possible representation of the prototype.

A limited research work is carried out on the transmission poles/masts. Task committee on steel transmission pole structures, ASCE Structural Division [1], has done a significant work on the subject matter. This report provides a uniform basis for the design and fabrication of steel pole structures. However, load deflection (P–Δ) analysis mentioning deflection limitation and compression capacity (buckling load) for non-prismatic members like tapered and elliptical polygonal poles etc. are not given in this report. Analysis aspects are introduced without reasonable details and are too brief to understand.

International Electrotechnical Commission (IEC) has also published a report (IEC-826) on loading and strength of overhead transmission lines [5 & 6]. Weather related loads and some of the special loading used for a pole are primarily based on the provisions of IEC 826 1991-94 (Swiss, Geneva). This report applies to overhead lines of nominal voltage above 45KV. ASCE Committee [2] has produced a report (ASCE Manual-91) on guyed transmission structures. Another publication of ASCE 1993 (ASCE Manual-52) provides a guide for design of Steel Transmission Towers that serves as a basis for the design of both guyed and self-supporting steel transmission towers [3]. Longitudinal unbalanced loads on transmission line structures were considered as given by EPRI (1978) [6].

Islam, A. Khan [10] carried out study on transmission towers. Various approaches to assess loads on conductors and structure using different codes of practices are described. Comparison of which is made and most appropriate technique for the assessment of wind

loading on towers is established for local conditions. Final year students of Session 1983-87 at University of Engineering and Technology, Lahore, made a study for their final year project on the design of 200 ft. high television lattice tower composed of steel skeletal members made of tubular section [11].

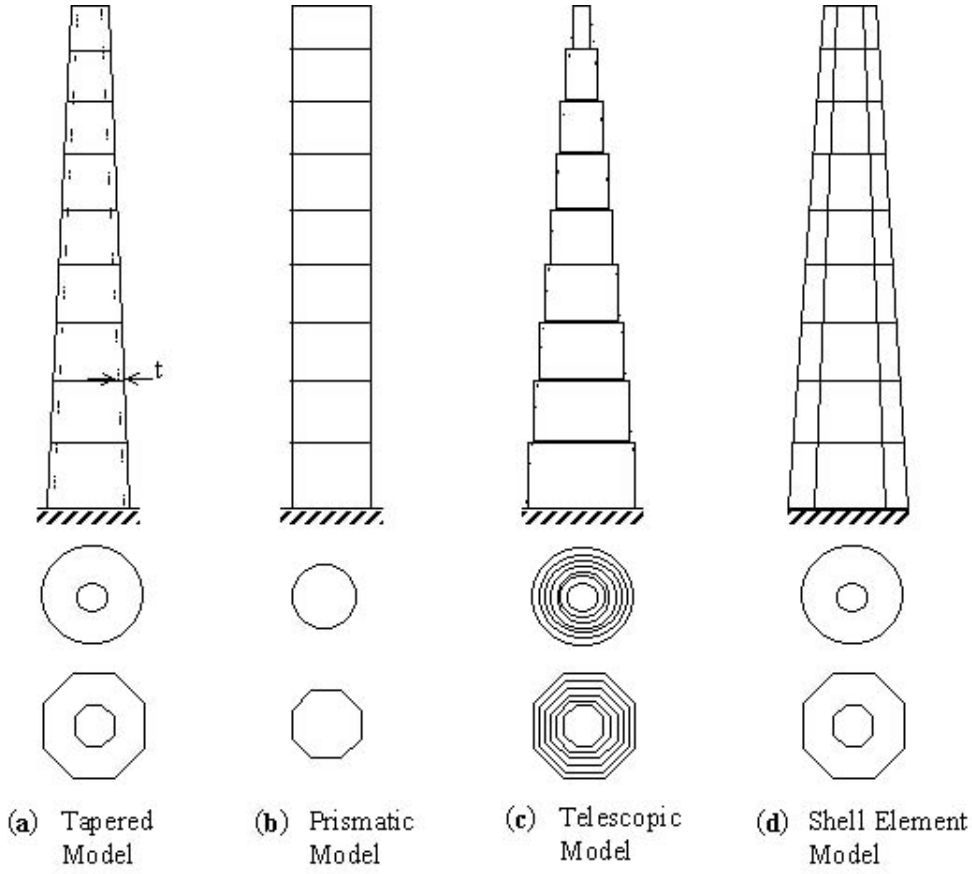

Figure 1. Analytical Models for Poles

The routine analysis of polygonal tubular (Fig 1a) mast executed by the designers is primitive and crude. This model has been improved to take care of secondary effects by the authors. Usually designers carryout the analysis considering the polygonal pole as a round skeletal member (Fig 1b). To incorporate the effect of taper, mast is modelled as telescopic tubular section in which cross section varies abruptly at different levels (Fig 1c). This approach is not realistic and hence needs verification due to non-representation of actual structure truly. Even if discretization is required, it should be done as in (Fig 1d) using shell elements in finite element method. The purpose of present study is:

- ✓ To elaborate the various loading cases/states to which a transmission structure is ever subjected in its whole life, e.g. high wind loading, reduced wind loading, construction and maintenance, erection and stringing loads, diagonal wind loads,

residual static loads and precamber loads.

- ✓ To establish the methodologies for the analysis of the mast that also incorporates the second order effects, which are necessary to be considered for such flexible structures.
- ✓ Recommendations for the most appropriate mast modelling technique for the future analysis and design.

2. ANALYSIS BASED ON TAPERED MODEL

Tapered model (Fig 1a) is developed in this paper to take care of secondary effects. This technique was evolved exclusively for tapered round and polygonal poles, however, it is equally good for prismatic section by inputting the shaft taper to be zero. This method is simple and convenient for formulation or automation in the form of in-house spreadsheets or computer programs having both the options of linear and non-linear analysis. Provisions for the local buckling stability can also be incorporated in this computer program. The results obtained from this method are in better agreement with the exact solution achieved from shell analysis employed in standard packages compared with those given by other methods. This is particularly true for pole segments having constant thickness. In case of variable thickness, each pole segment of constant thickness is treated separately and their results are summed up. This, however, becomes tedious and hence assumption of average thickness of all the segments is made. This simplifies the analysis but keeping the acceptable level of accuracy. Another advantage of this modelling technique is its in-sensitivity for the number of nodes unlike SAP90 and STAAD III models. Only loaded points, segment junctions and support points need to be considered in the analysis. It is further gratifying to note that the Tapered Model leads to conservative results compared with the exact solution.

The analysis technique is based on the uniformly tapered polygonal tubular mast model whose differential equations have been developed along with their solution. This is the most accurate representation of steel pole structure among all other methodologies, with the exception of mast analysis based on finite element method. However, the exact solution requires considerably large computer memory, time and efforts.

3. DIFFERENTIAL EQUATIONS FOR ELASTIC CURVE OF MAST AND SOLUTION

3.1 Deflection relationships for mast subjected to lateral loads

Consider a uniformly tapered hollow tubular polygonal or round (Pole) section with top dia D_t, base dia D_b and dia D_x at any distance x from the base as shown in Fig 2. It is subjected to gravity and lateral loads. Moment at distance x_1 from base due to lateral load P applied at distance L is

$$M = P\,(L - x_1) \tag{1}$$

From the Mohr's Second Theorem as given by Timoshenko [8], to calculate deflection δ_x

at a certain distance x from base, take the moment of differential area about section at distance x_1 from base which is:

$$M\, dx_1(x-x_1) = P(L-x_1)(x-x_1)\, dx_1 \tag{2}$$

Now, this differential area is integrated on the span from base to the point where deflection is to be determined i.e.

$$\delta_x = \int_0^x \frac{1}{EI} P(L-x_1)(x-x_1)dx_1 \tag{3}$$

where

L' = total pole length
L = height above base upto the point of application of P and S
P = Applied Lateral Load
S = Applied Compressive Load
E = Modulus of elasticity (Constt.)
k = pole taper
= $(D_b - D_t)/L'$
D_x = $D_t + (D_b - D_t)/L' \times x$
= $D_t + k\, x$
= $D_b - k\, x$
D_{x1} = $D_t + k\, x_1$
D_{x1} = $D_b - k\, x_1$
x = $(D_x - D_t)/k$

Hence second moment of area expression for above case becomes:

I = $C_i\, D_{xl}^3 t$ (variable along the pole length)

$$= C_i\,(D + k\, x_1)^3\, t = C_i(D_b - k\, x_1)^3\, t \tag{4}$$

C_i = Numerical multiplying factor for MOI expression
= $\pi/8$ for circular hollow tube and 0.411 for Dodecagonal tube.
D_x = Mean dia across flats (at a point where deflection δ_x is desired)
D_{x1} = Mean dia across flats at distance x_1 from base.
D_1 = Mean dia at the pt. Of application of load P.

Putting all the values in equation (3), we have

$$\delta_x = \frac{P}{C_i\, E\, t} \times \text{I G} \tag{5}$$

where

$$\mathrm{IG} = \int_0^x \left[x_1^2 - (L+x)x_1 + Lx\right](D_b - k\,x_1)^{-3}\,dx_1$$

$$= \frac{1}{k^3}\ln\frac{D_b}{D_x} - \frac{1}{2k^2}\left(\frac{x-L}{D_x} + \frac{x+L}{D_b}\right) - \frac{Lx}{2kD_b^2}$$

Hence,

$$\delta_x = \frac{P}{C_i E t}\left[\frac{1}{k^3}\ln(D_b/D_x) - \frac{1}{2k^2}\left(\frac{x-L}{D_x} + \frac{x+L}{D_b}\right) - \frac{Lx}{2kD_b^2}\right]$$

for $x \le L$

$$\text{At} \quad x = L, \ \delta_x = \delta_L \quad \text{and} \quad D_x = D_t$$

$$\delta_L = \frac{P}{C_i E t}\left[\frac{1}{k^3}\ln(D_b/D_t) - \frac{L}{k^2 D_b} - \frac{L^2}{2kD_b^2}\right] \tag{6}$$

$$\delta_x = \delta_L + \theta_L\,(x - L) \quad \text{for} \quad L \le x \le L' \tag{7}$$

From above equation, it is evident that for the determination of deflection at point above the point of application of load, elastic curve slope at the load point is needed.

From the Mohr's first theorem,

$$\theta_x = \int_{x_1=0}^{x_1=x} \frac{1}{EI} P(L - x_1)\,dx_1$$

$$= \frac{P}{C_i E t}\int_0^x (L - x_1)(D_b - kx_1)^{-3}\,dx_1 = \frac{P}{C_i E t} \times \mathrm{IG}$$

where

$$\mathrm{IG} = \int_0^x (L - x_1)(D_b - kx_1)^{-3}\,dx_1$$

$$= \frac{1}{2k^2}\left(\frac{1}{D_x} - \frac{1}{D_b}\right) - \frac{1}{2k}\left(\frac{x-L}{D_x^2} + \frac{L}{D_b^2}\right) \tag{8}$$

Hence the slope θ_x becomes

$$\theta_x = \frac{P}{2C_i E t}\left[\frac{1}{k^2}\left(\frac{1}{D_x} - \frac{1}{D_b}\right) - \frac{1}{k}\left(\frac{x-L}{D_x^2} + \frac{L}{D_b^2}\right)\right] \tag{9}$$

At x = L, $\theta_x = \theta_L$ and $D_x = D_t$ considering the constant diameter beyond L distance from the base, the above equation becomes

$$\theta_L = \frac{PL}{2C_i E t k D_b}\left[\frac{1}{D_t} - \frac{1}{D_b}\right] = \frac{PL}{2C_i E t k D_b}\left[\frac{D_b - D_t}{D_b D_t}\right] = \frac{PL^2}{2C_i E t D_b^2 D_t} \quad (10)$$

Similarly, if the pole is subjected to transverse moment M applied at distance x from base, displacement relationships can be established as follows:

From the Mohr's Second Theorem,

$$\delta_x = \int_0^x \frac{1}{EI} M(x - x_1)\, dx_1 \quad (11)$$

$$= \frac{M}{C_i E t}\left[\frac{1}{2k^2}\left(\frac{1}{D_x} - \frac{1}{D_b}\right) - \frac{x}{2kD_b^2}\right] \quad \text{for} \quad x \le L \quad (12)$$

At x = L, $\delta_x = \delta_L$ and $D_x = D_t$ the above equation becomes

$$\delta_L = \frac{M}{2C_i E t}\left[\frac{1}{k^2}\left(\frac{1}{D_t} - \frac{1}{D_b}\right) - \frac{L}{kD_b^2}\right] \quad (13)$$

$$\delta_x = \delta_L + \theta_L (x - L) \quad \text{for} \quad L \le x \le L' \quad (14)$$

To find the slope of elastic curve, θ, the given procedure may again the employed.

$$\theta_x = \int_{x_1=0}^{x_1=x} \frac{1}{EI} M dx_1$$

$$= \frac{M}{2C_i E t k}\left[\frac{1}{D_x^2} - \frac{1}{D_b^2}\right] \quad (15)$$

At x = L, $\theta_x = \theta_L$ and $D_x = D_t$, the above equation becomes

$$\theta_L = \frac{M}{2C_i E t k}\left[\frac{1}{D_t^2} - \frac{1}{D_b^2}\right] \quad (16)$$

The deflection and slope relationships discussed above give displacements and slopes due to bending caused by lateral loads (force and moment) only. The vertical loads further enhance these deflections due to second order P–Δ effects. When the deflection due to

bending is large and axial load produces bending stresses that cannot be neglected, the maximum stress is given by

$$f = P/A + (M + S\delta)\, c/I \tag{17}$$

where δ is the deflection of the pole. For axial compression, the moment Sδ should be given the same sign as M, and for tension, the opposite sign, but the minimum value of M+Sδ is zero. The deflection δ for axial compression and bending can be obtained by applying the basic moment curvature relationship.

$$M = EI\, d^2 y/dx^2 \tag{18}$$

and using M+Sδ in place of M [8&9]. It, however, may be closely approximated by

$$\delta = \frac{\delta_o}{1-\alpha} \text{ in which } \alpha = \frac{S}{P_E} \tag{19}$$

where

δ_o = deflection for the lateral loading alone (δ_x or δ_L – derived earlier)

P_E = Euler Critical buckling load for tapered pole considering elastic behaviour of the material.

To calculate the critical buckling compression capacity of tubular tapered members or any other non-prismatic member with variation of cross-section under a certain geometrical rule (e.g. hyperbolic variation etc.), the following approach can be employed.

A column of variable cross section, symmetrical with respect to the centre-line and having two axial planes of symmetry, is shown in Fig 3. The middle portion is of uniform cross section with its smaller moment of inertia equal to I_o. At the ends the cross section varies, and the smaller moments of inertia follow the expression below.

$$I = I_o\, (x/a)^m \tag{20}$$

For x = b, $I = I_o(b/a)^m$

For x = a, $I = I_o$

In above equation, x and a are distances from a fixed point and m is a number depending upon the type of column. When the middle portion is a solid cylinder and the ends are solid cones, I varies as the fourth power of x and m = 4 in the equation. When the column has a constant thickness in the direction perpendicular to the plane of section, the moments of inertia I with respect to axes parallel to the plane of the figure are proportional to x and m=1 in equation. (When the column consists of four angles connected by lattices of pyramidal shape, the cross-sectional area remains constant, and I can be taken proportional to x^2, so that m = 2 in the equation). Calculations made for m = 1, 2, 3, 4, show that the critical load as given by Timoshenko & Gere [9] within the elastic limit can be represented by the following expression:

$$P_E = \alpha \frac{E I_o}{(k)l^2} \tag{21}$$

in which α is a numerical factor depending upon the ratios h/l and I_l/I_o, where $I_I = I_o\,(b/a)^m$ is the moment of inertia of the end cross-section. The magnitudes of α for various ratios are given in a table [7]. It can be seen from the table that as the ratio h/L or the ratio I_l/I_o approaches unity the factor α approaches π^2 and the load value approaches the value for a prismatic bar.

Some Publications especially ASCE-72 [1] use another numerical factor that is basically derived from the α-factor (described above) called taper coefficient, which is denoted by P*.

For a uniformly tapered tubular pole as shown in the Fig 4,

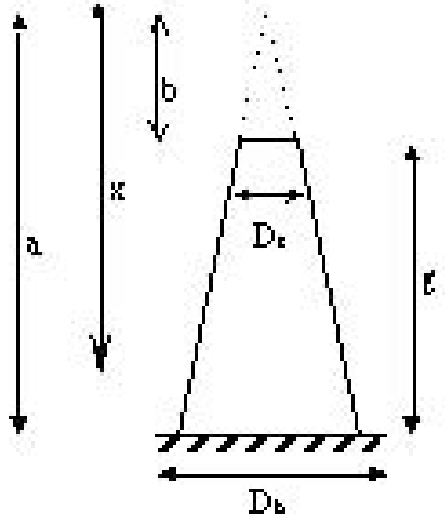

Figure 4. Uniformly Tapered Tubular Pole

I_o = I_b (at pole base level),
I_I = I_t (at pole top level)

The equation $I = I_o\,(x/a)^m$ gives:

$I_t/I_b = (b/a)^m$
$I_b/I_t = (a/b)^m$
$I_b = I_t\,(a/b)^m$

where $m = \log(I_b/I_t)/\log(a/b)$

Usually m ranges between 3 and 4 for steel polygonal tubular structures.

For geometry of Fig 4, $a/b = D_b/D_t$

$$\therefore\ m = \log(I_b/I_t)/\log(D_b/D_t) \tag{22}$$

$$\text{and} \quad I_b = I_t(D_b/D_t)^m \tag{23}$$

So for tapered pole Euler Buckling load becomes

$$P_E = \frac{\alpha E I_b}{(K l)^2} = \frac{\alpha E I_t \left(D_b / D_t\right)^m}{(K l)^2} \tag{24}$$

Comparing it with the general Euler formula for an equivalent prismatic member of same dimensions as of pole top that is multiplied by a coefficient P* to make it equal to P_E for tapered pole i.e.

$$P_E = P^* \frac{\pi^2 E I_t}{(K l)^2} \tag{25}$$

Where I_t is the moment of inertia at the top of the pole (based on D_t)

$$\therefore P^* = \frac{\alpha}{\pi^2}\left(D_b / D_t\right)^m \tag{26}$$

Hence, Euler buckling load for tapered pole section is:

$$P_E = P^* \times P_{E,top} \tag{27}$$

where

$$P_{E,top} = \frac{\pi^2 E I_t}{(K l)^2}$$

If the thickness of steel pole segments is not uniform and varies abruptly from segment to segment and this abrupt variation is not according to certain mathematical rule, formulation of variable thickness expression is quite difficult. A convenient solution for this problem is to assume average thickness for all pole segments. This assumption is sufficiently close to the prototype and further its results are confirmed from ASCE-72 (1978) [2].

4. RESULTS

This section presents a design example that demonstrates the application and use of mast analysis principles, tapered modelling approach and its most of the formulae recommended.

The results are compared with the load and stress analysis output by standard computer programs and packages employed. A 220 KV Double Circuit Tangent Pole has been taken for the study. Two-dimensional front view of this pole along with selected dimensions is shown in Fig 5. The technical data to be considered for the design of selected steel tubular pole is as under:-

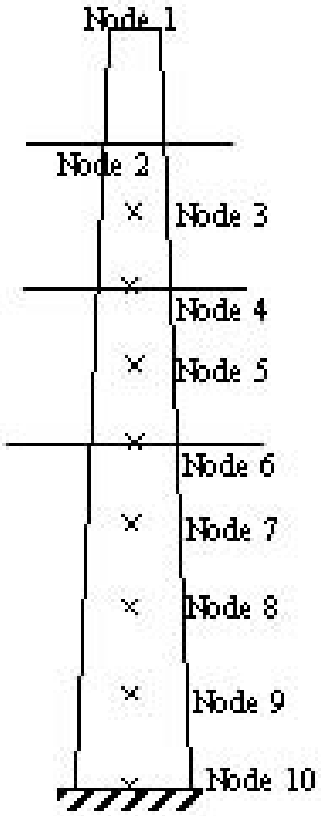

Figure 5. Dimensions of The Selected 220 KV Twin Bundle Tangent Pole

Pole	Characteristics	Dimensions
1)	Deflection angle	0 – 2 deg.
2)	Ruling span	180 m
3)	Wind span	200 m
4)	Maximum weight span	250 m

5. CONDUCTOR

ACSR "RAIL", 45/7 strands, Tensile Strength (TS) of 11874 kg., twin bundled per phase.

5.1 Shieldwire (OPGW)

Aluminium Clad Steel (Equivalent to 7/8 AWG with 30% Conductivity) with OPGW construction. 70mm^2 cross-section, 11.4 mm diameter, 8000 kg strength and unit weight of 0.45 kg/m.

5.2 Safety Factors

1) Erection, Stringing and Maintenance Loads = 1.5
2) Pole Dead Weight= 1.2

Table 1. Results Obtained From Primary (First Order) Analysis (Primary Analysis Results are same for all modelling approaches) Critical Load Case # 1

Node No.*	Vertical Distance (m) from bot to top	Axial Force ΣP_x ton	Transfer Shear ΣP_y ton	Longi. Shear ΣP_z ton-m	Resultant Shear ΣP_{yz}	Trans. Moment ΣM_z ton-m	Longi. Moment ΣM_y ton-m	Resultant Moment ΣM_{yZ} ton-m	Torsion ΣM_x ton-m
1	32.250	0.120	0.402	0.000	–	0.000	0.000	0.000	0.000
2	28.050	1.976	5.612	0.000	–	1.688	0.000	1.688	0.000
3	25.582	2.806	6.862	0.000	–	15.541	0.000	15.541	0.000
4	22.800	4.662	12.072	0.000	–	34.628	0.000	34.628	0.000
5	20.750	4.662	12.072	0.000	–	59.376	0.000	59.376	0.000
5	20.750	4.662	12.072	0.000	–	59.376	0.000	59.376	0.000
6	17.550	6.518	17.282	0.000	–	98.006	0.000	98.006	0.000
7	15.065	8.866	19.165	0.000	–	140.950	0.000	140.950	0.000
8	10.200	8.866	19.165	0.000	–	234.190	0.000	234.190	0.000
8	10.200	8.866	19.165	0.000	–	234.190	0.000	234.190	0.000
9	7.833	12.556	21.303	0.000	–	337.056	0.000	337.056	0.000
10	0.000	12.556	21.303	0.000	–	440.006	0.000	440.006	0.000

*** The node numbers and their locations are shown in Figure 5.**

6. POLE DESIGN LOADS

Wind velocity = 150 km/hr.

Wind load on conductor, shield wire and pole are to be calculated in accordance with IEC-826 [5].

6.1 Load Cases Considered

Four load cases were considered for the analysis of the pole. Case 1 (Load Condition # 1) represents transverse wind, with all wires intact. In Case 2 (Load Condition #2), diagonal wind at 45° is considered with all wires intact. Longitudinal load due to wind on conductor and shield wire is taken equal to 30% of the transverse wind condition. Case 3 is a model of the stringing conditions. The stringing tension is considered to be 10% of tensile strength of conductor and shield wire. This case is further divided into four load conditions as under:

Table 2. Results of Uniformly Tapered Polygonal Tubular Model Considering Second Order Effects (Non-Linear Analysis) Under Critical Load Case #1

Node No.	Ht from base m	Axial Force ΣP_x ton	Trans. Shear ΣP_y Ton	Longi. Shear ΣP_z ton	Resultant Shear ΣP_{yz} ton	Trans. Moment M_z ton-m	Longi. Moment M_y ton-m	Resultant Moment* M_{yZ} ton-m	Torsion M_x ton-m
1	32.250	0.12	0.40	0.00	0.40	0.000	0.000	0.000	0.000
2	28.050	1.98	5.61	0.00	5.61	1.756	0.000	1.756	0.000
3	25.582	2.81	6.86	0.00	6.86	16.242	0.000	16.242	0.000
4	22.800	4.66	12.07	0.00	12.07	36.269	0.000	36.269	0.000
5	20.750	4.66	12.07	0.00	12.07	62.060	0.000	62.060	0.000
5	20.750	4.66	12.07	0.00	12.07	62.060	0.000	62.060	0.000
6	17.550	6.52	17.28	0.00	17.28	102.108	0.000	102.108	0.000
7	15.065	8.87	19.17	0.00	19.17	146.340	0.000	146.340	0.000
8	10.200	8.87	19.17	0.00	19.17	242.136	0.000	242.136	0.000
8	10.200	8.87	19.17	0.00	19.17	242.136	0.000	242.136	0.000
9	4.833	12.56	21.30	0.00	21.30	346.563	0.000	346.563	0.000
10	0.000	12.56	21.30	0.00	21.30	450.111	0.000	450.111	0.000

* **Resultant Moment** $M_{yz} = \sqrt{M_y^2 + M_z^2}$

a) Shield wire-stringing condition with 6 phases intact. Only longitudinal load without wind (Load Condition # 3),
b) Shield wire stringing only with no wind (Load Condition # 4),
c) Shield wire intact, 5 phases intact and any one phase in stringing condition, with no wind (Load Condition # 5),
d) Stringing of shield wire along with stringing of any one phase (Load Condition # 6).

Case 4 (Load Condition # 7) is a broken wire condition showing any phase and shield wire broken with 5 phases intact. Maximum tension in conductor is taken equal to 50% of every day tension.

Summary of the results for different load cases including critical load case #1 are given in tabular form as under:

EW = Earth wire
Top X = Top cross arm
Top X-L = Top left cross arm
Top X-R = Top right cross arm
Mid X = Middle cross arm, Mid X-L & Mid X-R
Bot X = Bottom cross arm, Bot X-L & Bod X-R
MS Start = Middle segment start
BS Start = Bottom segment start

Table 3. Base Reactions For All Load Cases For Uniformly Tapered Polygonal Tubular Mast Model

Sr. No.	Load Case #	Axial Force	Shear Force (kg)			Bending Moment (kg-m)			Torsion	Remarks
		P(kg)	S_T	S_L	S_R	M_T	M_L	M_R	Tor. (kg-m)	
1	Case 1	12556	21303	0	21303	450087	0	450087	0	A.C
2	Case 2	12556	12179	14107	18637	25039	297884	388974	0	
3	Case 3a	15400	0	1200	1200	0	40460	40460	0	B
4	Case 3b	7048	0	1200	1200	0	39043	39043	0	
5	Case 3c	15400	0	3351	3351	0	97804	97804	13293	B
6	Case 3d	8440	0	4551	4551	0	134901	134901	13293	
7	Case 4	12109	0	2172	2172	0	64545	64545	6712	

Note: Axial force is downward and includes the wt of the portion above ground for the pole shaft times the appropriate load factor, in addition to the concentrated vertical loading.

Key to the special remark

A Indicates load case with Max. Resultant Over-turning Moment.

B Indicates load case with Max Axial Force.

C Indicated load case with Max Resultant Shear.

Hence, Load Case #1 is critical for Anchor Bolts & Base Plate as it leads to Max. Res. Shear & Overturning Moment

Table 4. Comparison Of Total Resultant Moment (Primary & Secondary) M_{yz} Under Critical Load Case # 1

Node No.	Location	Ht above base m	Tapered Model ton-m	SAP 90 Frame El. ton-m	STAAD III Frame El. ton-m
1	EW	32.250	0.000	0.000	0.000
2	Top X	28.050	1.756	1.750	1.750
3	Atc1+WTS	25.582	16.242	16.160	16.160
4	Mid X	22.800	36.269	36.040	36.030
5	TS End	20.750	62.060	61.620	61.630
5	MS Start	20.750	62.060	61.620	61.630
6	Bot X	17.550	102.108	101.380	101.390
7	Atc2+WBS	15.065	146.340	145.260	145.260
8	MS End	10.200	242.136	240.630	240.620
8	BS Start	10.200	242.136	240.630	240.620
9	Atc3+WBS	4.833	346.563	344.780	344.780
10	Base	0.000	450.111	448.180	448.170

Notes: Axial & Shear forces being identical are not shown in comparison.

Table 5. Comparison Of Resultant Second Order Moments For All Models Under Critical Load Case # 1

Node No.	Location	Ht above base m	Tapered Model ton-m	SAP 90 Frame El. ton-m	STAAD III Frame El. ton-m
1	EW	32.250	0.000	0.000	0.000
2	Top X	28.050	0.068	0.060	0.060
3	Atc1+WTS	25.582	0.701	0.610	0.610
4	Mid X	22.800	1.640	1.410	1.400
5	TS End	20.750	2.684	2.250	2.260
5	MS Start	20.750	2.684	2.250	2.260
6	Bot X	17.550	4.102	3.380	3.380
7	Atc2+WBS	15.065	5.390	4.400	4.400
8	MS End	10.200	7.946	6.430	6.420
8	BS Start	10.200	7.946	6.430	6.420
9	Atc3+WBS	4.833	9.507	7.670	7.670
10	Base	0.000	10.104	8.170	8.160

Table 6. Comparison Of Resultant Lateral Deflections δ_{Yz} For All Models Critical Load Case # 1 $\left(\delta_{yz} = \sqrt{\delta_y^2 + \delta_z^2}\right)$

Node No.	Location	Ht above base m	Tapered Model (m)	SAP 90 Frame El. (m)	STAAD III Frame El. (m)
1	EW	32.250	2.456	2.104	2.103
2	Top X	28.050	1.893	1.593	1.592
3	Atc1+WTS	25.582	1.572	1.309	1.304
4	Mid X	22.800	1.238	1.013	1.013
5	TS End	20.750	1.014	0.826	0.826
5	MS Start	20.750	1.014	0.826	0.826
6	Bot X	17.550	0.709	0.578	0.277
7	Atc2+WBS	15.065	0.512	0.418	0.418
8	MS End	10.200	0.224	0.183	0.183
8	BS Start	10.200	0.224	0.183	0.183
9	Atc3+WBS	4.833	0.048	0.040	0.040
10	Base	0.000	0.000	0.000	0.000

Table 7. Summary of Design Based on the Analysis

Segment	Length m	Lapped Length	Ht. Of Seg. bot.	Bot joint #	Top dia Cm	Bot.dia cm	Thick cm	K m/m	Connect. between	Joint type	Overlap provided	Theoretical Length (m)
TS	11.50	11.50	20.75	5	20.000	56.800	0.635	0.03200	TS-MS	SLIP	0	0
MS	11.50	10.55	10.20	8	55.530	89.290	0.953	0.03200	MS-BS	SLIP	0.95	0.87
BS	11.65	10.20	0.00	10	87.384	120.000	1.032	0.03198	BS-B.PL	WELD	1.45	1.36
		32.25			Average thickness =		0.873	cm				

TS = Top Segment. MS = Middle Segment BS = Bottom Segment

Table 8. Stress Analysis Of Pole Shaft Obtained from the Analysis using Tapered Model

Node No.	Location	Ht m	$f_A=P_x/A$	For a=0	For a=15deg		For a=45deg		For a=75deg		For a=90	f_b	f_a+f_b	f_{vy}-direct	f_{vz}-direct	f_y-tor.	Combined (kg/cm^2)		Add. FOS=
			Kg/cm^2	$f_{by}=M_zC_y/I$	$f_{by}=M_zC_y/I$	$f_{bz}=M_yC_z/I$	$f_{by}=M_zC_y/I$	$f_{bz}=M_yC_z/I$	$f_{by}=M_zC_y/I$	$f_{bz}=M_yC_z/I$	$f_{bz}=M_yC_z/I$	kg/cm^2	kg/cm^2	kg/cm^2	kg/cm^2	kg/cm^2	F_{act}	F_{allow}	$F_{allow}=F_{act}$
1	EW	32.250	3.03	0	0	0	0	0	0	0	0	0	3	20.63	0.00	0.00	3	4570	1508
2	Top X	28.050	29.46	330	319	0	233	0	85	0	0	330	359	169.99	0.00	0.00	359	4570	12.72
3	Atc1+WTS	25.582	33.71	1975	1907	0	1396	0	511	0	0	1975	2008	167.52	0.00	0.00	2008	4570	2.28
4	Mid X	22.800	45.96	2961	2860	0	2094	0	766	0	0	2961	3007	241.83	0.00	0.00	3007	4570	1.52
5	TS End	20.750	40.59	3946	3812	0	2790	0	1021	0	0	3946	3987	213.58	0.00	0.00	3987	4570	1.15
5	MS Start	20.750	27.84	2802	2706	0	1981	0	725	0	0	2802	2829	146.45	0.00	0.00	2829	4570	1.62
6	Bot X	17.550	32.77	3259	3148	0	2305	0	844	0	0	3259	3292	176.54	0.00	0.00	3292	4570	1.39
7	Atc2+WBS	15.065	39.71	3700	3574	0	2616	0	958	0	0	3700	3740	174.38	0.00	0.00	3740	4570	1.22
8	MS End	10.200	32.71	4145	4004	0	2931	0	1073	0	0	4145	4178	143.65	0.00	0.00	4178	4570	1.09
8	BS Start	10.200	30.90	4010	3874	0	2836	0	1038	0	0	4010	4041	135.70	0.00	0.00	4041	4570	1.13
9	Atc3+WBS	4.833	36.50	3986	3851	0	2819	0	1032	0	0	3986	4023	125.83	0.00	0.00	4023	4570	1.14
10	Base	0.000	31.76	3915	3781	0	2768	0	1013	0	0	3915	3947	109.49	0.00	0.00	3947	4570	1.16

FOS available for worst case = 1.09 > 1.0OK

Table 1 gives the results of primary (first order) analysis of the mast. Since effect of deflections in increasing the moments is ignored in the first order analysis, the results are same for all the models. For brevity, results obtained from analysis for critical loading case (case # 1) are only reproduced. The shear, moments and axial forces shown are at the 10 nodal points selected on the main pole body at locations mentioned in this table.

Table 2 shows the results of secondary (geometrically non-linear) analysis of tapered mast model for the critical load case. The shear and axial forces are same as in Table 1 (first order analysis) but the moments are increased due to P-Δ effects. Since critical loading case is transverse wind only, longitudinal shears i.e. ΣP_z are zero and consequently longitudinal moments ΣM_y are also zero. Since there is no unbalanced longitudinal load on cross-arms for this load case, applied torque (ΣM_x) is also zero. The rate of increase in moment due to second order effect varies along the pole height. There is an increase of 2.3% in primary moment due to P-Δ effects at the base of pole.

Table 3 gives the summary of support reactions at base of pole for all the seven loading cases computed using the Tapered model. These reactions are to be used in the design of base plate, anchor bolts, stiffeners (if any) for base plate, and the concrete foundation. Some of the loading cases give maximum axial load and others maximum shear force, maximum bending moment, or maximum twisting moment (torsion). This has been shown by the remarks in the table.

Table 4 depicts the relative accuracy and precision of results achieved from various analytical models. This gives a glance at the non-linear lateral resultant moments, at different levels of pole, for all the models for the critical loading case (load condition # 1). At each level, there is a slight difference in values of various models, which is due to the assumptions employed in the development of each model. The moments for the Tapered Mast Model has a close match with the finite element models prepared for the comparison and verification purpose. Thus, this close agreement authenticates the accuracy of the proposed model.

The P-Δ effects (second order moment) computed using the three models for the critical load case are given in Table 5.. Since, the SAP-90 Model and STAAD III Models are based on the same reference diagram (Telescopic/Stepped model, Fig-1c), their solutions are almost the same. Tapered Model results are close to the FEM results. Comparison cannot be made directly with the Shell Element Model results, as its output is not of the form of that of skeletal model. One has to take mean of the respective moments of the shell elements meeting at a node. The axial pole deflections are too small (negligible) and are not compared.

Table 6 gives the resultant lateral deflections of all models including shell element model for the critical load case. The deflection varies from a maximum value of 2.456m for tapered mast model to a minimum of 2.080m for Shell Element model. This is a large deflection and confirms the recommendation for the steel pole to be treated as a flexible structure. Since, the example structure is tangent type, the lateral deflections are produced by the transverse wind only (contribution to transverse load due to a deflection angle of 2 deg is negligible). This deflection is momentary and pole raking or cambering is not needed. The most accurate and exact model amongst all is the shell element model. SAP-90: Frame Model and STAAD-III: Frame Model results are sufficiently close to the shell

element model and thus provide a good alternate solution to shell element modelling. The proposed Tapered Model gives a little bit more deflection due to the assumption of uniform thickness of all pole segments in the analysis of example pole. If the Tapered Model formulae are individually applied to each segment, then the deflections will perhaps be more close to that of Shell Model. This is because Tapered Model gives more true representation of the prototype than stepped model.

The dimensions of pole components (design summary) that satisfy all types of applied loading without overstressing its any part are recorded in Table 7. Various specifications recommend different amount of lap for splice joint. Here it has been taken equal to 1.5 times the largest diameter of female end. The provided lap is more than the specified one. The diameters shown in the table are outer across-flats. The number of segments have been kept as minimum as possible to avoid the wastage of material of lap splices. The connection between all the segments is through splice joint, however, pole and base plate are connected through welding.

Table 8 gives an overview of pole shaft stresses induced at its various levels due to internal stress resultants (obtained from non-linear analysis of Tapered Model) for critical load case. Allowable stresses for axial, flexure, shear torsion and their combination have been taken from design specifications. Because of the superior torsional stiffness of closed tubular section, allowable stresses are not reduced for lateral torsional buckling. However, local buckling criteria have been used to avoid any local instability due to large flat width/thickness ratio. Polygon corners (located at angles of 15, 45 & 75 deg etc.) might be critical for combination of bi-axial moments, axial load, torsion etc., therefore, all these are checked. Since in the load case considered only transverse moment is present, maximum bending stress is found at angle of zero degree (i.e. a=0). Additional FOS (i.e. FOS in addition to the specified factor of safety) varies along the pole height. The most critical point is the end of middle section (junction of middle and bottom section) as it has minimum FOS of 1.09. It is notable that despite both segments are subject to same loading at their junction, BS (bottom segment) has more FOS (i.e. 1.13) even though it has lesser diameter at the junction than the diameter of MS (female end). This is due to increased thickness of BS from 9.53mm to 10.32mm that increases the stiffness (cross-sectional properties) increasing in turn the additional FOS.

7. CONCLUSIONS

The study of steel transmission pole is carried out using tapered model along with SAP 90 and STAAD-III models. The following important conclusions are drawn from this work:

- In steel pole structures, the maximum allowable stress on the pole is related to the width to thickness ratio for structures with polygonal cross-sections and by diameter to thickness ratios for structures with circular cross-sections.
- Limiting the defection to one or one half percent (1 or ½%) of the structure height under construction loading can eliminate the need for back guying structures during construction. For appearance, limiting deflections to five or ten percent (5 or 10%) of the structure height under maximum loading can keep a pole in a position, which

seems to an observer almost straight. Another technique that is used to keep steel pole structure appearance aesthetically pleasing is to camber or rake the structures before erection. Cambering or raking makes the structure initially deformed so that when load is applied to the structure, it tends to become straight or appears less deformed.

- The package programs have limitations: SAP90 can only perform analysis and there is no provision for design. STAAD-III has no general database for design of polygonal tubular tapered structures. The subject structure is non-prismatic and, while designing it as a skeletal member, regular variation of cross-sectional properties cannot be incorporated in these softwares. Therefore, designers model it as a telescopic Tubular polygonal mast having regular cross-section that abruptly changes at intervals.
- The shell element and uniformly tapered model are the best representation of the prototype. Therefore, for mast analysis and design either by a software/method truly representing the prototype should be used or as an alternate of SAP90 and STAAD-III frame element models may be employed with substantial number of nodes, giving stepping at each node, to achieve their close coherence with the prototype. Moreover, one has to be cautious regarding the local or overall stability while using these softwares, as they are incapable to check this for non-prismatic structures.
- Stiffness of the structure is reduced by almost 10% when it is designed as a skeletal structure ignoring the effect of continuum, however, skeletal simulation for analysis purpose is accepted being handy, simple and on conservative side. STAAD-III has in-built option for non-linear and P-Δ analysis, whereas SAP90 may conduct the linear analysis only. Therefore, for the subject pole, 2^{nd} order analysis on SAP90 was done using the deflected geometry of the structure.
- Sometimes, client restricts the base diameter due to space or other constraints that indirectly limit the amount of taper. In such a case, the design output is only the wall thickness of pole segments that is adjusted to satisfy all the design criteria.
- Poles, being flexible structures, are subjected to considerably large deflections e.g. 2 to 4m. The major contribution in these deflections is from lateral loads, which are further increased by vertical loads due to P-Δ effects. For the tangent poles, this large deflection will be infrequent and occasional in its entire life span (i.e. when it is subjected to worst possible high wind/lateral loading). Hence, these large deflections need not to be controlled. For angle poles, however, lateral loads are not casual which cause permanent large lateral deflections. There are various ways to deal with the problem of these large deflections. Pre-cambering and adjustment of the anchor bolts by setting base plates of poles in inclined position opposite to the likely displaced form of pole are two common techniques.
- Most of the poles consist of 3 to 4 segments. A single pole segment usually has an economical and optimal length of 12m. The minimum thickness of material used for poles is usually 6mm.
- Design of the polygonal mast considering it a round tube is not realistic. ASCE-72 [1] gives entirely different criterion for elastic stability of round, hexdecagonal, dodecagonal and octagonal or fewer-sided tubes.
- The overturning moments of transmission poles are usually too high in comparison to vertical loads. The resultant force fall considerably far from the pole centre. A

shallow foundation, therefore, is not usually designed for poles due to avoid overturning.

- Torsional shear stress calculations for the pole are done using membrane analogy by some designers and as a regular hollow shaft by the others. The latter is supported by ASCE [1].
- While modelling the pole as shell element, membrane action has been found dominant and plate bending stress resultants are too small and may be neglected. Hence, pole can be modelled as membrane elements without loss of much accuracy with the added advantage of lesser computer memory and time requirements.
- In case of tubular tapered pole, moment of inertia varies along the member length. To calculate the Euler buckling load, P_E, for such members or any other non-prismatic member with varying cross-section under a certain geometrical rule (e.g. hyperbolic variation etc.), a Taper Coefficient has been derived in this paper. This coefficient involves a factor α to be obtained from Roark et al. [7]. In Tapered Model, Lateral deflections are magnified for vertical loads by an empirical factor $1/(1 - P/P_E)$. This coefficient is the key part of this model.
- Using Mohr's theorems, 2nd order non-homogeneous differential equations have been developed and solved. Numerical integration can also be employed using Rung Kutta method.
- Deflections for Shell model are least due to loss of stiffness by $1/(1 - \nu^2)$ (=10% for $\nu \approx 0.3$) in skeletal models. Flexural rigidity for frame element is $EI=Et^3/12$ and $EI=Et^3/12(1 - \nu^2)$ for plate element.
- The efficacy of the developed analytical technique i.e. tapered model is evident from close agreement of results obtained from this method and those achieved from the exact method based on finite element method using a standard package. Further, the developed model is simple to use even with hand calculations conveniently or by employing MS Excel spreadsheet on a personal computer.

REFERENCES

1. ASCE "Design of Steel Transmission Pole Structures", ASCE Manual No. 72, ASCE, 2nd Edition, New York, 1990.
2. ASCE Design of Steel Transmission Pole Structures, ASCE, New York, 1978.
3. ASCE Guide for Design of Steel Transmission Towers, ASCE Manual No. 52, ASCE, 2nd Edition, New York, 1993.
4. Dinnik A.N., Bull Engrs., Westrick Ingenerov; 1927 (Russian language).
5. IEC–826 (1991-04). Loading and Strength of Overhead Transmission Lines, International Electrotechnical Commission. 2nd Edition.
6. EPRI, Longitudinal Unbalanced Loads on Transmission Line Structures, EPRI EL-643, Project 561. GAI Consultants, Inc., Monrovoeville, Pennsylvania, 1978.
7. Roark et al., Formulas for stress and strain, 5th Edition, McGraw Hill Book Company, New York.
8. Timoshenko, S., Strength of Material Part I & II (Advanced), 3rd Edition, Van Nostrand

Reinhold Company, 1956.
9. Timoshenko, S. and Gere, J. M., Theory of Elastic Stability, McGraw-Hill Book Company, New York.
10. Islam, A. Khan. University of Engineering and Technology, Lahore, Pakistan. (M.Sc. Thesis, 2000).
11. UET, Lahore Student Session 1983-1987. Design of 200 ft. High Transmission Tower, (Final Year B.Sc. Thesis, 1987).